Catena 206 (2021) 105501

Contents lists available at ScienceDirect

Catena

journal homepage: www.elsevier.com/locate/catena

Oxygen footprint: An indicator of the anthropogenic ecosystem changes

Dongliang Han [a], Jianping Huang [a,*], Lei Ding [b], Xiaoyue Liu [b], Changyu Li [b], Fan Yang [b]

[a] Collaborative Innovation Center for Western Ecological Safety, Lanzhou University, Lanzhou 730000, China
[b] College of Atmospheric Science, Lanzhou University, Lanzhou 730000, China

ARTICLE INFO

Keywords:
Oxygen footprint
Anthropogenic climate change
Drylands
Modelling
Risk

ABSTRACT

Drylands are one of the most sensitive areas to anthropogenic climate change and are projected to experience accelerated expansion throughout the end of this century. However, the responses of drylands degradation to anthropogenic ecosystem changes remain unclear. This study proposes a new perspective of the 'oxygen footprint', defined as the ratio between oxygen consumption and oxygen production, which could be regarded as an indicator in evaluating the effects of anthropogenic climate change on global dryland ecosystems. A global distribution of the trend of oxygen footprint in response to climate change indicators and the transformations for ecosystem functioning is presented. The response of oxygen footprint to human activities and global warming is projected to enhance in the 21st century. Under a high emissions scenario (RCP8.5), linear regression analysis between oxygen footprint and other indicators shows oxygen footprint to increase with the increase of air temperature, precipitation, potential evapotranspiration and dryland areas, respectively. Our study suggests that when oxygen production is unsustainable combined with oxygen consumption, this scenario will accelerate the degradation of dryland ecosystem, with fundamental and negative consequences for the capacity of drylands to supply essential ecosystem services.

1. Introduction

Drylands, areas where precipitation (PRE) is <65% of potential evapotranspiration (PET) demand (Yao et al., 2020), cover approximately 45% of emerged lands, and support more than 35% of the world's population (Huang et al., 2016a; Berdugo et al., 2020). Increasing aridity is driven by climate and environmental changes, and by anthropogenic activities such as land use and land cover changes (Cheng et al., 2016; Huang et al., 2017a; Guan et al., 2019). Degradation and desertification are pervasive in drylands due to the rapid population growth, economic development and urbanization impacts, especially in developing countries (Huang et al., 2017a). Because most dryland vegetation cover is sparse, which is associated with the weakening of plant productivity, soil fertility and water storage capacity, dryland ecosystems are substantially more fragile (Reynolds et al., 2007).

However, many studies found that drylands were greening (revealed a close connection between oxygen activity and vegetation primary production) during recent years (Fensholt et al., 2012; Piao et al., 2015; Chen et al., 2019). Using normalized difference vegetation index data from 1981 to 2007, Fensholt et al. (2012) reported an increasing trend in vegetation greenness over global drylands. Using different leaf area index data and ecosystem models over the last 30 years, Piao et al. (2015) further analyzed key drivers of greening trends and concluded that CO_2 fertilization is an important factor driving vegetation greenness. Subsequent studies based on medium-resolution and fine-resolution satellite data (Chen et al., 2019) have shown the key role of land use/cover history, including agricultural intensification and afforestation (the conversion of a place where there are no or few trees to forests through planting trees), in enhancing vegetation greenness.

The greening indicator, together with aridity and warming, represents credible evidence of the eco-environmental effect of anthropogenic climate change (Piao et al., 2020). Carbon emissions have long been considered to play a crucial role in the drivers or mechanisms of anthropogenic climate change. For example, as economic development has progressed rapidly, more fossil fuel has been consumed, producing substantial amount of CO_2. The excessive emission of CO_2 plays an

Abbreviations: AI, Aridity index; AT, Air temperature; CMIP5, Coupled model intercomparison project phase five; CO_2, Carbon dioxide; GHG, Greenhouse gas; NEP, Net ecosystem productivity; NPP, Net primary productivity; O_2, Oxygen; O_F, Oxygen footprint; PET, Potential evapotranspiration; PRE, Precipitation; RCP, Representative concentration pathway; R_h, Soil heterotrophic respiration; SOC, Soil organic carbon.

* Corresponding author.
E-mail address: hjp@lzu.edu.cn (J. Huang).

https://doi.org/10.1016/j.catena.2021.105501
Received 23 July 2020; Received in revised form 28 April 2021; Accepted 27 May 2021
Available online 4 June 2021

Table 1
. The relationship of oxygen and dryland ecosystems.

Indicators	Description
Climate	Climate change has been linked to the rapid increase of CO_2 content but has not been extensively considered to the changes in O_2 content. In fact, the O_2 content, because of its contribution to atmospheric density and mass, affects the optical depth of the atmosphere, is considered a key factor in climate forcing (Poulsen et al., 2015). Under low O_2 content and a reduced-density atmosphere, shortwave scattering by clouds and air molecules is less frequent, resulting in a substantial increase in surface shortwave forcing (Poulsen et al., 2015). Through feedbacks involving latent heat fluxes to the marine stratus clouds and atmosphere, surface shortwave forcing drives raises land surface temperature and enhances greenhouse forcing (Poulsen et al., 2015).
Vegetation	Vegetation greening (Zhu et al., 2016), which is defined as a statistically significant increase in seasonal or annual vegetation greenness at a location resulting, including increases in species composition, plant density, etc., as compelling evidence for anthropogenic climate change (Piao et al., 2020). For instance, the greening in China is from croplands (32%) and forests (42%), but in India is minor contribution from forests (4.4%) with mostly from croplands (82%) (Chen et al., 2019). In comparison with forest, the large contribution of agricultural activities may be correlated more strongly with a higher leaf-level maximum carboxylation rate, the maximum monthly gross primary productivity and maximum photosynthetic capacity (Huang et al., 2018b). However, the greening phenomenon, could leading to destroy the natural structure of soil and water loss due to evapotranspiration (Huang et al., 2017a).
Soil	Soil organic carbon (SOC), as a key determinant of soil fertility, plays an important role for climate regulation and food production (Jansson and Homfmockel, 2020), is determined by the balance between C outputs through microbial decomposition and C inputs from plants, with these processes occurring interactively in nature (Chen et al., 2019). However, these key processes in the soil that are associated with CO_2, O_2 and water balance may have been broken, owing to their high sensitivity to anthropogenic activities (e.g., tillage). Tillage could destroy the soil mineral-organic associations and aggregate occlusion, i.e., SOC stability (Lehmann and Kleber, 2015), and enhance the capacity of microbial decomposition of SOC and soil heterotrophic respiration activity (Yan et al., 2018), and thus reduce the SOC content in cropland (Yu et al., 2017).
Water	Water deficiency is characterized by its spatial distribution that the global endorheic system experienced a widespread water loss of ~106.3 Gt yr^{-1} during 2002–2016, attributed to comparable losses in groundwater, soil moisture and surface water (Wang et al., 2018). Decreasing soil fertility linked to water deficiency is resulting in an expanse of soil degradation and desertification, and drylands are projected to increase by 11–23% over the next century (Huang et al., 2016a). The changes in water availability can have profound and lasting effects on C turnover, plant activity and microbial metabolic, ultimately affecting plant photosynthetic capacity. Because dryland ecosystems are globally distributed, it is difficult to generalize oxygen responses to dryland degradation across regions.

important driving role in warming in drylands, particularly in high greenhouse gas emission scenarios (Huang et al., 2017a; Huang et al., 2017b). The fluctuations in CO_2 are closely negatively correlated with changes in O_2, and the ratio in the amplitude of the changes in CO_2 and O_2 mole fractions are in line with the ratio from fossil fuel burning (Keeling, 1988).

Unlike CO_2, O_2 is not considered a key factor in climate forcing due to its ignorable contribution to the radiative forcing of the atmosphere (Poulsen et al., 2015). However, through its impact on atmospheric density, O_2 directly impacts solar optical depth, and thus enhances greenhouse forcing and raises land surface temperature (Poulsen et al., 2015). Drylands ecosystem may be much more sensitive to O_2 than for CO_2. On the one hand, solar radiative forcing provides a larger land surface forcing than greenhouse forcing; on the other hand, because CO_2 decreases radiative cooling, it is fewer effective than solar forcing in driving changes in the amount, variability and intensity of PRE (Poulsen et al., 2015). Therefore, a decrease in O_2 may have amplified CO_2-driven anthropogenic climate change.

A better understanding of the responses of dryland ecosystems to the changing oxygen under future climate scenarios is urgently needed. In the Anthropocene (Crutzen, 2002), the variation of atmospheric O_2 concentration is dominated by vegetation primary production and anthropogenic activities, which are closely related to dryland ecosystems (Table 1). Here, we propose a new concept of the 'oxygen footprint', which is defined as statistically significant increase or decrease in oxygen at the corresponding timescales. The oxygen footprint (O_F) not only results from natural and anthropogenic variability but also responds to the climate through biogeophysical and biogeochemical processes. For instance, given that decrease carbon storage in soil, such as through tillage and irrigation, could promote CO_2 emissions and accelerate soil water loss (Zhang et al., 2015; Yu et al., 2017), ultimately affecting soil fertility and vegetation oxygen production capacity.

In this study, we first analyze and discuss the variations in O_F using observational data combined with model simulations. Subsequently, we explore what are the responses of dryland ecosystems to the changing O_F, according to the identifies phases characterized by climate change and dryland expansion. Finally, the paper is concluded by identifying important challenges for future work.

2. Methods

Globally, drylands refer to the areas where the ratio of total annual PRE to PET (aridity index, AI) is below 0.65, and regions where the annual averaged PRE-is below 600 mm (Hulme, 1996; Feng and Fu, 2013; Huang et al., 2016b). According to the values of AI, drylands can be further classified as dry sub-humid ($0.5 \leq AI < 0.65$), semi-arid ($0.2 \leq AI < 0.5$), arid ($0.05 \leq AI < 0.2$) and extremely arid ($AI < 0.05$) areas. The extremely arid areas are the driest, and followed by arid, semi-arid and dry sub-humid areas in four types of drylands. For observation, the temperature, PRE and PET data set from 1948 to 2005 developed by the Climatic Prediction Center (Chen et al., 2002; Fan and Dool, 2008). For simulations, the simulation data (2006–2099) under the representative concentration pathway (RCP)4.5 and RCP8.5 scenarios from 20 global climate models of Coupled Model Intercomparison Project, Phase 5 (CMIP5) are shown in Taylor et al., 2012. More details are available from previous publication (Huang et al., 2020).

2.1. Method of estimating the oxygen production

In the drylands, based on the terrestrial net primary productivity (NPP), net ecosystem productivity (NEP) and soil heterotrophic respiration (R_h), the oxygen production is derived from the CMIP5 models results. The ensemble means of the CMIP5 models address the uncertainty in inter-model variability and provide better predictions than any individual model (Huang et al., 2016a). Thus, the ensemble means of CMIP5 models (Huang et al., 2018a) were selected based on the criterion that they provide terrestrial NPP, NEP and R_h. Because the CMIP5 historical simulations end in 2005, we extended them to ~2100 by splicing them with the corresponding RCP4.5 and RCP8.5 scenarios (Marvel et al., 2019). As a result, oxygen respiration can be expressed as:

$$6H_2O + 6CO_2 \rightarrow C_6H_{12}O_6 + 6O_2 \quad (1)$$

where $C_6H_{12}O_6$ is the approximate composition of terrestrial organic matter; NEP refers to the amount of NPP remaining after including the consumption of R_h. Subsequently, the NEP was calculated as follows:

$$NEP = NPP - R_h \quad (2)$$

because the molar mass of oxygen is 32 g per mole and that of carbon

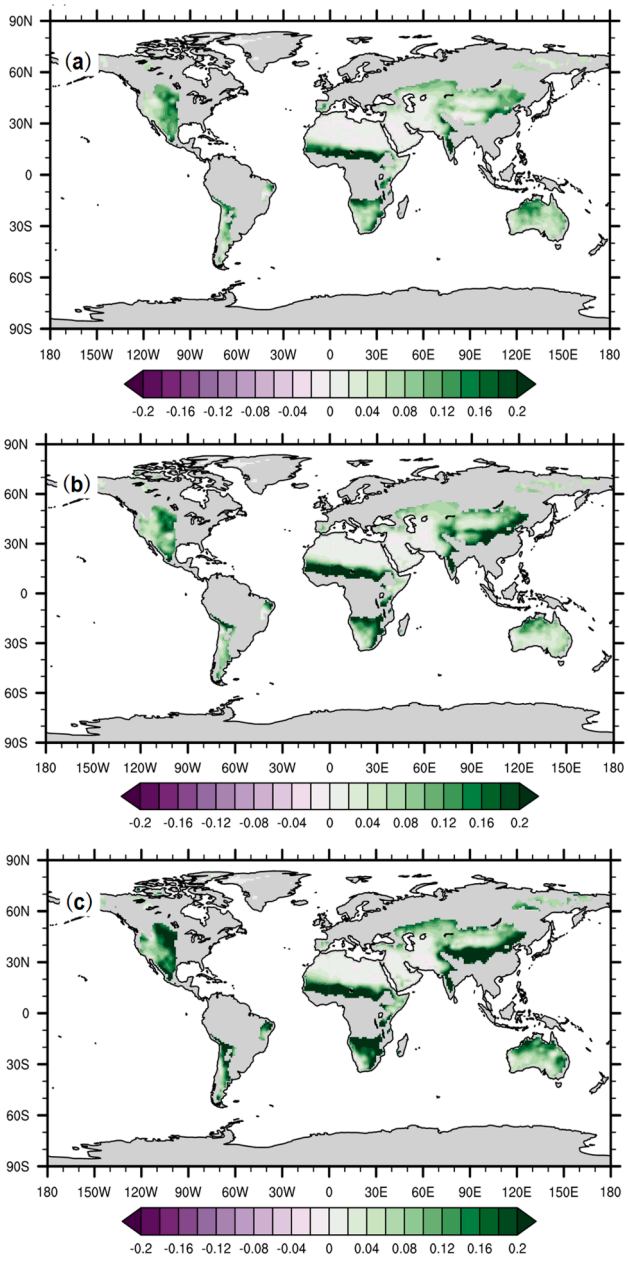

Fig. 1. CMIP5-based investigate of the oxygen production (kg m^{-2}) over drylands. (a) The mean historical distribution of oxygen production in 1975–2005 (30 years). (b) and (c) represent the mean oxygen production from 2069 to 2099 (30 years) relative to the historical under the RCP4.5 and RCP8.5 scenario, respectively.

is 12 g per mole. The ratio is 2.667. Finally, we further calculated the net amount of oxygen based on the following linear regression:

$$O_2 = NEP \times 2.667 \quad (3)$$

Further details of these methods for oxygen production analyses have previously been published (Huang et al., 2018a).

2.2. Method of estimating oxygen consumption

In this study, oxygen consumption is mainly driven by fossil fuel combustion, human respiration, livestock respiration, and wildfires.

Fossil fuel combustion. We obtained data of CO_2 emissions (1751–2013) from the carbon dioxide information analysis center (CDIAC data on ESS-DIVE, available at http://cdiac.ess-dive.lbl.gov/). The estimation of O_2 content by fossil fuel combustion was converted according to the methods and criteria in Steinbach et al. (2011). Owing to the different fuel mix in each country, the oxidative ratio can vary over temporal and spatial characteristics of scale. Therefore, the consumption of oxygen by fossil fuel combustion as follows:

$$C_{FF} = M_{oxygen} \times \sum_{i=1}^{4} \frac{E_{FFi}}{M_C} \times ratio_i \quad (4)$$

where C_{FF}, M_{oxygen}, and M_C are the annual oxygen consume content (Gt oxygen per yr), the relative molecular mass of oxygen (32 g per mol), and carbon (12 g per mol), respectively. E_{FFi} is the *i*-th species carbon emissions from fossil fuel combustion (Gt carbon per yr). The $ratio_i$ is the molar ratio of O_2:C when the *i*-th fuel is completely burned.

Human respiration. To estimate the oxygen content of human

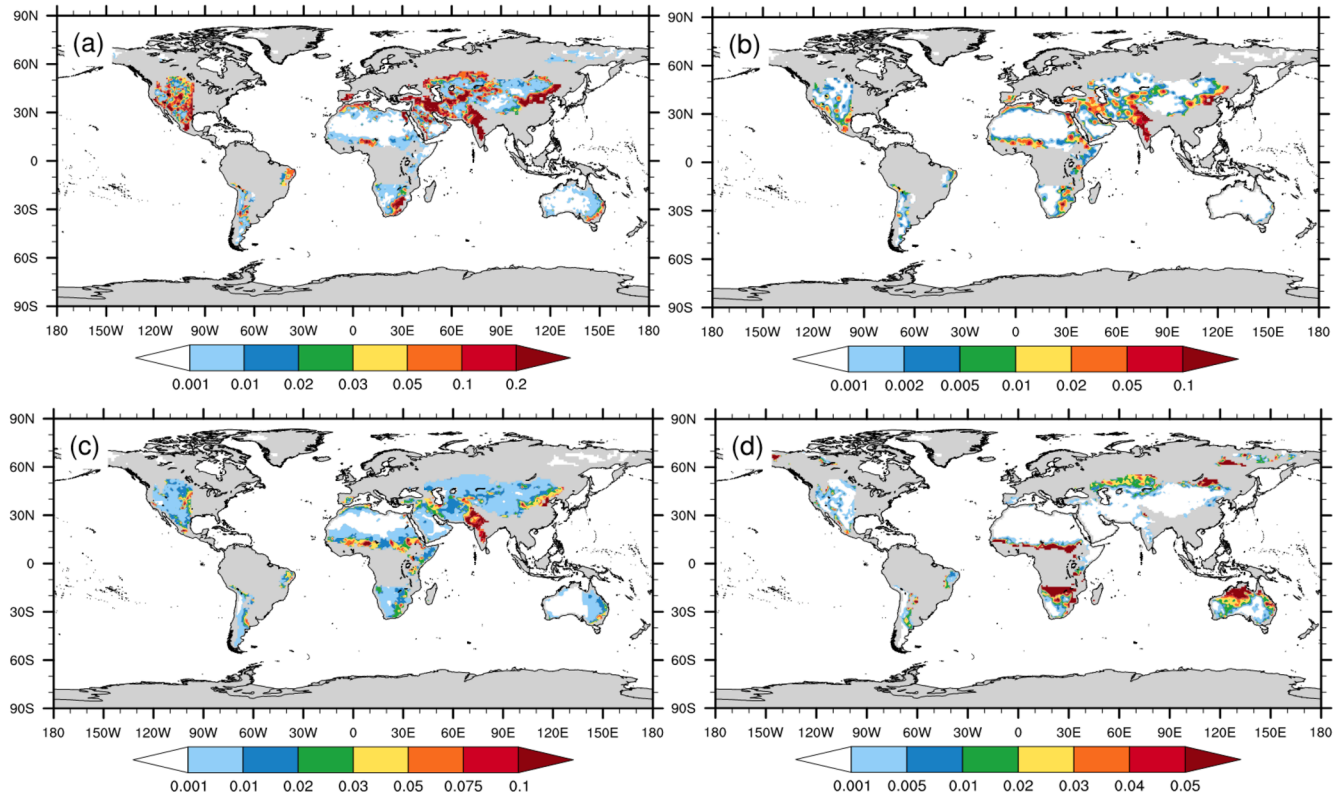

Fig. 2. The distribution of the mean oxygen consumption (kg m^{-2}) from 2000 to 2013 over drylands. (a), (b), (c) and (d) show fossil fuel combustion, human respiration, livestock respiration and wildfires, respectively.

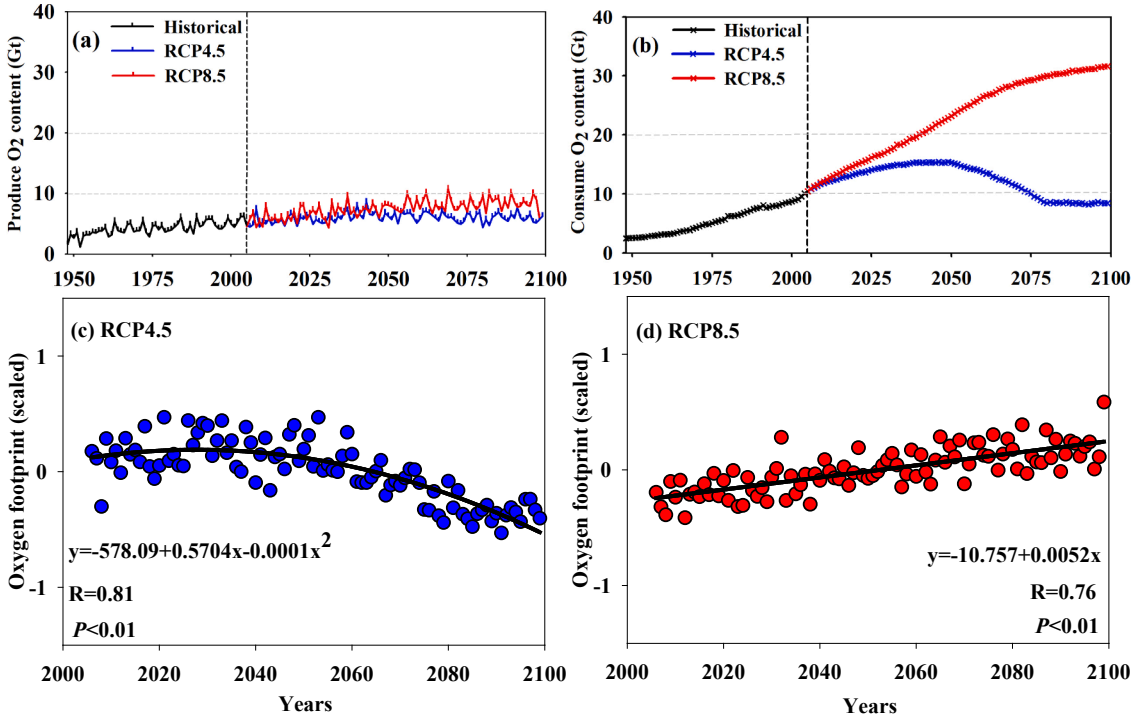

Fig. 3. The trend of oxygen footprint. (a) and (b) represent the changes in oxygen production and oxygen consumption under historical (black, 1948–2005), RCP4.5 (blue, 2006–2099) and RCP8.5 scenarios (red, 2006–2099), respectively. (c) and (d) represent the changes in the oxygen footprint under the RCP4.5 (blue) and RCP8.5 (red) scenarios over drylands from 2006 to 2099, respectively.

respiration by the end of the twenty-first century, all datasets were downloaded and analyzed from the population of the word version 4 (http://sedac.ciesin.columbia.edu/). If a man works 8 *h* with an oxygen consumption rate of 1.0 L oxygen per min and rests for the remaining 16 *h* with an oxygen consumption rate of 21.0 L oxygen per *h* in a day (the consumption of oxygen is approximately 1.17 kg, that is, 816 L per day for an adult). Thus, we calculated the total consumption of oxygen by human respiration as follows:

$$C_{HR} = TOP \times C_d \times 365 \quad (5)$$

where C_{HR} is the annual oxygen consumption through human respiration (Gt oxygen per yr), TOP is the total population, and C_d is the per capita oxygen consumption content in a day (kg oxygen per day).

Livestock respiration. We used the livestock of the world version 2.09 to analyses the consumption of oxygen from major livestock, including cattle, chickens, ducks, goats, pigs, and sheep. Previous studies (Huang et al., 2018a; Liu et al., 2020), applying the basal metabolism rate (BMR), have estimated that the annual oxygen consumption of livestock using the following equation:

$$BMR = 3.43M^{0.75} \quad (6)$$

where BMR (ml oxygen per h) is the rate of energy expenditure per unit time by endothermic animals at rest and can be reported in ml oxygen per min, M is the animal's mass (g). We then determined the total consumed oxygen content for each mammal using the cumulative approach as follows:

$$C_{LR} = \sum_{i=1}^{6} P_i \times BMR_{di} \times 365 \quad (7)$$

where C_{LR} is the annual oxygen consumption of livestock (Gt oxygen per yr), P_i is the total number of *i*-type livestock, and BMR_{di} is the mean daily oxygen consumption of the *i*-type livestock (kg oxygen per day).

Wildfires. Wildfires generally include natural and human-induced fires. We calculated the consumption of oxygen from fire by the global fire emissions database (GFED), version 4, and ranges from 1997 to 2016 (van der Werf et al., 2017). The six fire types (savanna fires, tropical forest fires, temperate forest fires, peatland fires, boreal forest fires, and agricultural waste burning) that were used in this study are available from satellite information on fire activity and vegetation productivity at http://www.globalfiredata.org. The molar ratio of O_2:CO_2 is 1.1 ± 0.1, owing to the combustion products are all organic (Liu et al., 2020). We calculated the consumption of oxygen by fire as follows:

$$C_{wildfires} = M_{oxygen} \times \sum_{i=1}^{6} \frac{DM_i \times CC_i \times EF_i}{M_C} \times 1.1 \quad (8)$$

where $C_{wildfires}$ is the oxygen consumed (Gt oxygen per yr), *i* indicates the type of fire, DM_i is the mass of the *i*-th fire type emitted (kg dry matter per yr), CC_i is the percentage of carbon in the *i*-type fire dry matter, and EF_i is the emissions factor of the *i*-th fire type C. M_{oxygen} and M_C is the relative molecular mass of oxygen (32 g per mol) and carbon (12 g per mol), respectively.

Further details of these methods for oxygen consumption analyses have previously been published (Liu et al., 2020).

2.3. Oxygen footprint calculations from simulations

The O_F as an indicator of dryland degradation that integrates changes in oxygen production and oxygen consumption. The CMIP5 was used to analyze the O_F based on oxygen production and oxygen consumption for 2006–2099 under the RCP4.5 and RCP8.5 scenarios. The O_F results were standardized by calculating the difference of individual simulates from the mean of all simulates and divided by the range of all simulations (a_i-$\bar{a}$)/(maximum(a)-minimum(a)). We calculated the O_F as follows:

$$O_F = O_c / O_p \quad (9)$$

where O_F is the oxygen footprint, O_c and O_p is oxygen consumption and oxygen production yearly from 2006 to 2099, respectively. All statistical analyses and charting work were performed using SPSS statistics 17.0, SigmaPlot 10.0, and Edraw Mind Map 7.9.

3. Results and discussion

3.1. Oxygen footprint

Oxygen footprint refers to a state in which anthropogenic ecosystem changes can indicate eco-environmental stability, associated with the terrestrial oxygen production and consumption drivers. However, continuing global warming and enhanced human activities pose a threat to oxygen footprint. Thus, knowledge of how climate change and human disturbances will affect changes in oxygen footprint in the future is essential for adaptation and protection strategies.

3.1.1. Changes in the oxygen production

The state-of-the-art climate process model-derived historical (1975–2005) oxygen production over the global drylands is shown in Fig. 1a. For comparison, we also show the trends in oxygen production of the RCP4.5 (Fig. 1b) and RCP8.5 (Fig. 1c) scenarios for the future period of 2069–2099. Notably, the oxygen production content for the two scenarios in all drylands indicates an increase at the end of the twenty-first century, particularly in the greenhouse-gas-dominated RCP8.5 scenario (Fig. 3a). The oxygen production content is higher for RCP8.5 than for RCP4.5 for four reasons in response to climate change.

First, rising CO_2 fertilization. The content of CO_2 is the substrate for photosynthesis, plays a significant role in oxygen production, increased CO_2 content can stimulate photosynthetic pathway (Farquhar and Sharkey, 1982) by accelerating the rate of carboxylation reaction of Rubisco (ribulose-1,5-bisphosphate carboxylase oxygenase); this oxygen production process is well known as the 'CO_2 fertilization effect'. Additionally, increases in atmospheric CO_2 contents can also enhance vegetation productivity by partially reducing stomatal conductance, resulting in enhanced water use efficiency while increased canopy temperatures (Keenan et al., 2013). Rising atmospheric CO_2 is the major driver of vegetation greening linked to stimulating oxygen production, accounting for approximately 70% of the global leaf area index trend (Piao et al., 2020). Regrettably, the strength of the CO_2 fertilization increases oxygen production linked to vegetation productivity can be limited by nutrient (Reich and Hobbie, 2013), extreme weather events (Gray et al., 2016) and water availability (Reich et al., 2014), particularly in dryland areas.

Second, increasing temperature and precipitation. Although rising atmospheric CO_2 content plays the dominant driver of oxygen production, anthropogenic warming (e.g., fossil fuel burning) and partial trends in PRE-are also the important factors of oxygen production. Using the dynamic global vegetation models, Piao et al. (2020) indicated that the positive impacts of warming, primarily from a warmer temperature, which is supported by the evidence of the greening (enhance photosynthesis) trend over more than 55% of the northern high latitudes. Additionally, in water-limited dryland ecosystems, changes in PRE, reflecting trends from anthropogenic warming, are suggested as the important driving factor of oxygen production. For instance, the 'greening Sahel' (Herrmann et al., 2005), one of the early examples of vegetation greening promotes oxygen production, is major driven by increases in atmospheric PRE-after a severe drought. PRE-plays a significant role in vegetation greenness is further supported through analyses of long-term field surveys and recent satellite measurements (Dardel et al., 2014; Brandt et al., 2019).

Third, expanding land use. Human land use in shaping the oxygen production exerts a considerable. In drylands, areas where intensive

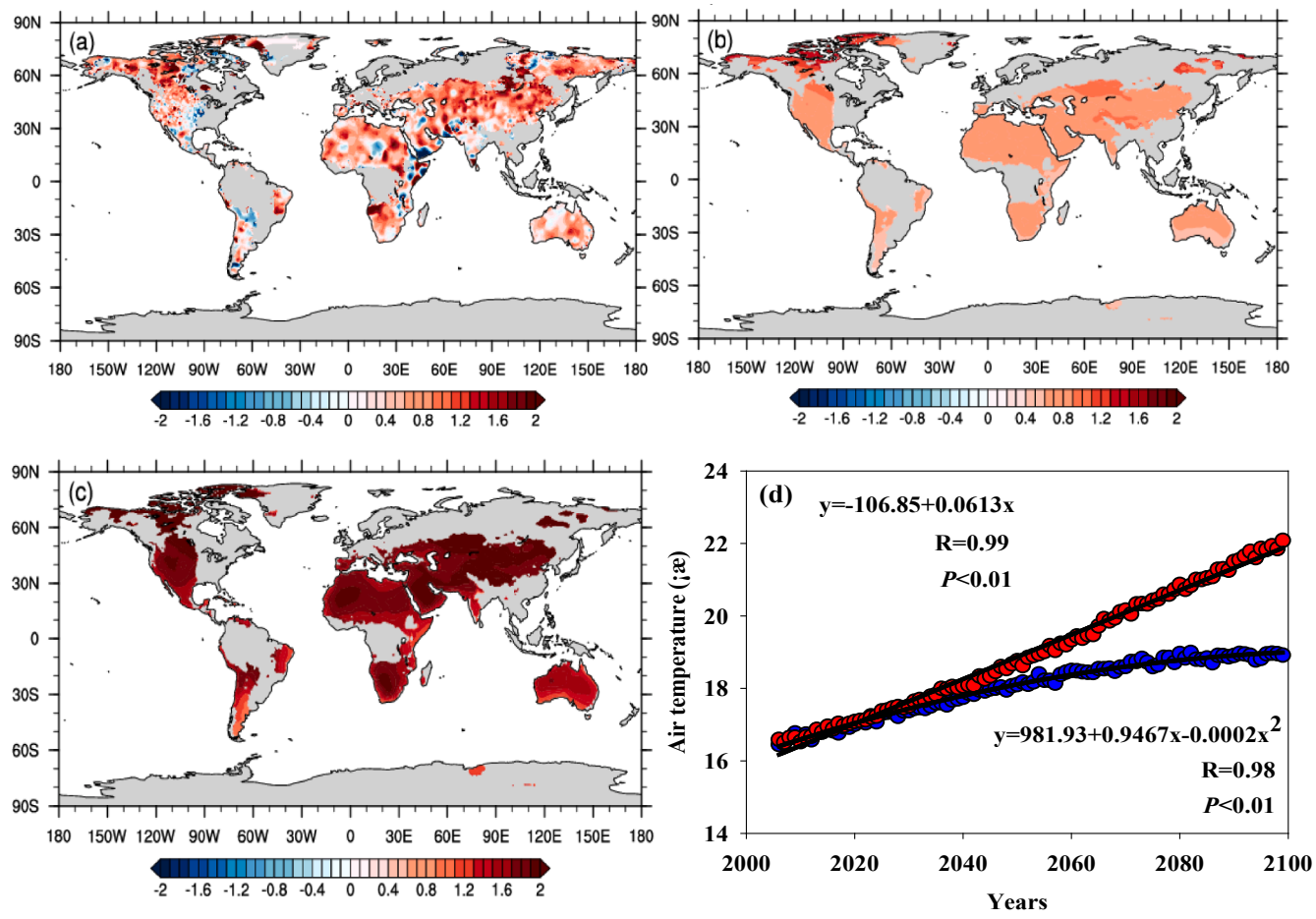

Fig. 4. Global distribution of the trend of air temperature (℃ 30 yr^{-1}) under the historical (a, 1948–2005), RCP4.5 (b, 2006–2099) and RCP8.5 (c, 2006–2099). Fig. d shows that temporal variation of mean annual air temperature in RCP4.5 (blue) and RCP8.5 (red), respectively.

afforestation is linked to a pronounced local increasing in oxygen production. However, planting trees in drylands increased the potential risk of soil water deficiency, owing to the trees deplete the soil water to compensate for the inadequate atmospheric PRE, and the effects of increasing depletion of soil water often become apparent many years later (Cao, 2008). In addition, agricultural intensification with a higher photosynthetic capacity than other biomes (Huang et al., 2018b), owing to multiple fertilizers, irrigation, and cropping contributes considerably to oxygen production. Unfortunately, this phenomenon is likely to disappear soon since the cropland associated with oxygen production in drylands could destroy the protection of soil aggregates to soil organic carbon such as tillage, and decrease the groundwater such as irrigation, and subsequently accelerate the land degradation and desertification.

Fourth, enhancing nitrogen deposition. Anthropogenic changes in the rate, amount, and distribution of nitrogen deposition can influence oxygen production. Nitrogen fertilization is extensively used to improve soil nitrogen availability and increase plant photosynthesis and vegetation primary production (Xia and Wan, 2008). Nitrogen addition on leaf number, size, and density was significant in almost all vegetation functional types (Huang et al., 2018b) and subsequently plays an indiscernible driving role in oxygen production at the global scales. However, nitrogen deposition processes linked to climate warming are highly managed by humans, so the difference in eco-environmental contributions in croplands is uncertain (Huang et al., 2018b). Based on this, future research priorities, including better representation and measurement of processes such as plant whole, root, stem, and leaf nitrogen uptake and allocation (Zaehle et al., 2014).

3.1.2. *Changes in the oxygen consumption*

Anthropogenic changes have contributed the most to oxygen consumption with fossil fuel combustion accounting for 70.68% of oxygen consumption, followed by wildfires (11.78%), livestock respiration (9.97%), and human respiration (7.57%) from 2000 to 2013 over drylands as shown in Fig. 2 (s). Oxygen consumption is extremely sensitive to rapid economic and societal development, especially in developing countries. Developing countries linked to global dryland ecosystems play a vital role in oxygen consumption, owing to continuing oil developments and a rapidly growing population in both rural and urban (Huang et al., 2017a). The oxygen consumption content is much stronger for RCP8.5 than for RCP4.5 (Fig. 3b) for three reasons in response to climate change.

Firstly, rapid population growth. Rapidly growing population will exacerbate the risk of greenhouse gas (GHG) emissions soon in developing countries (Huang et al., 2017a). This is because, increasing population is often associated with human activities (e.g., agricultural waste burning) and plays a key role in dryland oxygen and climate change (Table 1). Using CMIP5 transient CO_2 concentration increase to 2 × CO_2 concentration simulations that respond to GHG forcing, Fu and Feng (2014) found that the increase in the PET averaged over land is about 5.3% per degree of the ocean-mean surface air temperature (AT) increases, whereas PRE-increased at a rate of 1.7% per degree. Therefore, the ratio of PRE/PET (i.e., AI) decreases by about 3.4% per degree, resulting in a drier climate. The increased GHG emissions that have occurred in drylands is closely related to the rapid oxygen consumption. Additionally, Poulsen et al. (2015) showed that low oxygen

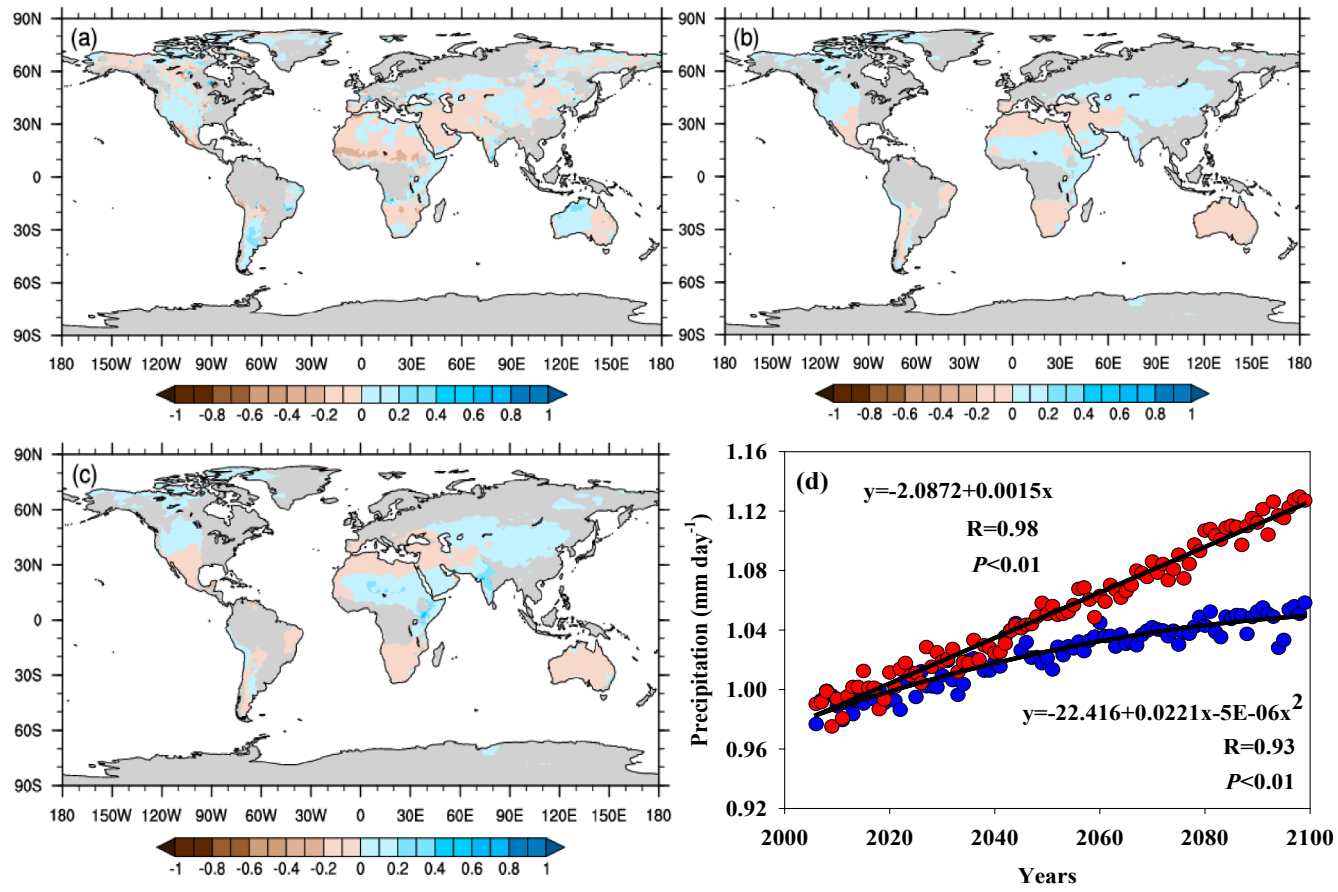

Fig. 5. Global distribution of the trend of precipitation (mm day^{-1} 30 yr^{-1}) under the historical (a, 1948–2005), RCP4.5 (b, 2006–2099) and RCP8.5 (c, 2006–2099). Temporal variation of mean precipitation is shown for RCP4.5 (blue) and RCP8.5 (red) in the Fig. d, respectively.

consumption influences on atmospheric density, leading to a substantial increase in solar forcing, enhances GHG forcing, and raises the global surface temperature. Thus, oxygen consumption is closely correlated with GHG forcing and solar forcing.

Secondly, accelerate economic development. As economic development has progressed rapidly (e.g., industry), more fossil fuels have been consumed as a source of energy for mining and transportation (Barnett and O'Neill, 2010; Mackey et al., 2013), driving oxygen consumption and producing substantial anthropogenic aerosols (Huang et al., 2017a; Huang et al., 2018a). Aerosol emissions are an anthropogenic radiative forcing (Lin et al., 2018). For example, black carbon is emitted in a variety of combustion processes, rapidly removed from the atmosphere by deposition, and alters the melting of snow and ice cover (Bond et al., 2013). This is because, light-absorbing particles in snow can significantly increase the amount of absorbed solar radiation and reduce snow albedo and produce warming (Bond et al., 2013). However, using model outs from CMIP5, Li et al. (2015) found that anthropogenic aerosols influenced on the temperature and exhibited greater contributions over the semi-humid/humid regions than over the arid-semiarid regions. Using three sets of ensemble simulations from the Community Earth System Model, Lin et al. (2018) showed that aerosol changes exert a small effect on global AI due to the offsetting impact of PRE and PET.

Thirdly, urbanization. Human activities have a prominent influence on regional environment and climate by altering temperature, moisture and energy exchange between land surface and atmosphere, for example, cities (Huang et al., 2017a). Cities are places where substantial consumption of various resources such as oxygen as well as where an increased course of urbanization such as automobile use, industrial operations or space heating have led to the development of 'urban heat island' (Oke, 1987), affecting the land surface properties. Smaller leaf areas would reduce transpiration by plant stomata and increase the surface albedo, further intensify drought (Taylor et al., 2002). The changes in land surface properties constitute important factors contributing to the observed reduction of PRE (Junkermann et al., 2009). Also, using a climate model (CSIRO Mk3L) coupled with a land surface scheme (Community Atmosphere Biosphere Land Exchange model), Avila et al. (2012) showed that human-induced changes in temperature extremes are not merely influenced by increasing CO_2 (or decreasing O_2); by contrast, land surface property changes may amplify the effect of GHG forcing (or solar forcing).

3.1.3. *Changes in the oxygen footprint*

According to the above results, O_F is driven by oxygen production and oxygen consumption under RCP4.5 and RCP8.5 scenarios (Fig. 3c-d), represents extremely credible evidence of anthropogenic climate change. The results highlight that when oxygen production (e.g., plant, soil, and water) would become unsustainable, and then would be combined with oxygen consumption (e.g., population growth, economic development, and urbanization), this scenario would accelerate the degradation of dryland ecosystem (Table 1 and Figs. 1–3). Therefore, O_F can not only alert us to climate crises (e.g., GHG forcing or solar forcing) but can also warn us about disasters (e.g., desertification) to take proactive action and mitigate their impacts. Our results suggest that the response of dryland ecosystem degradation to O_F can be organized into two phases, including climate change phase (Figs. 4–6) and dryland expansion phase (Fig. 7s).

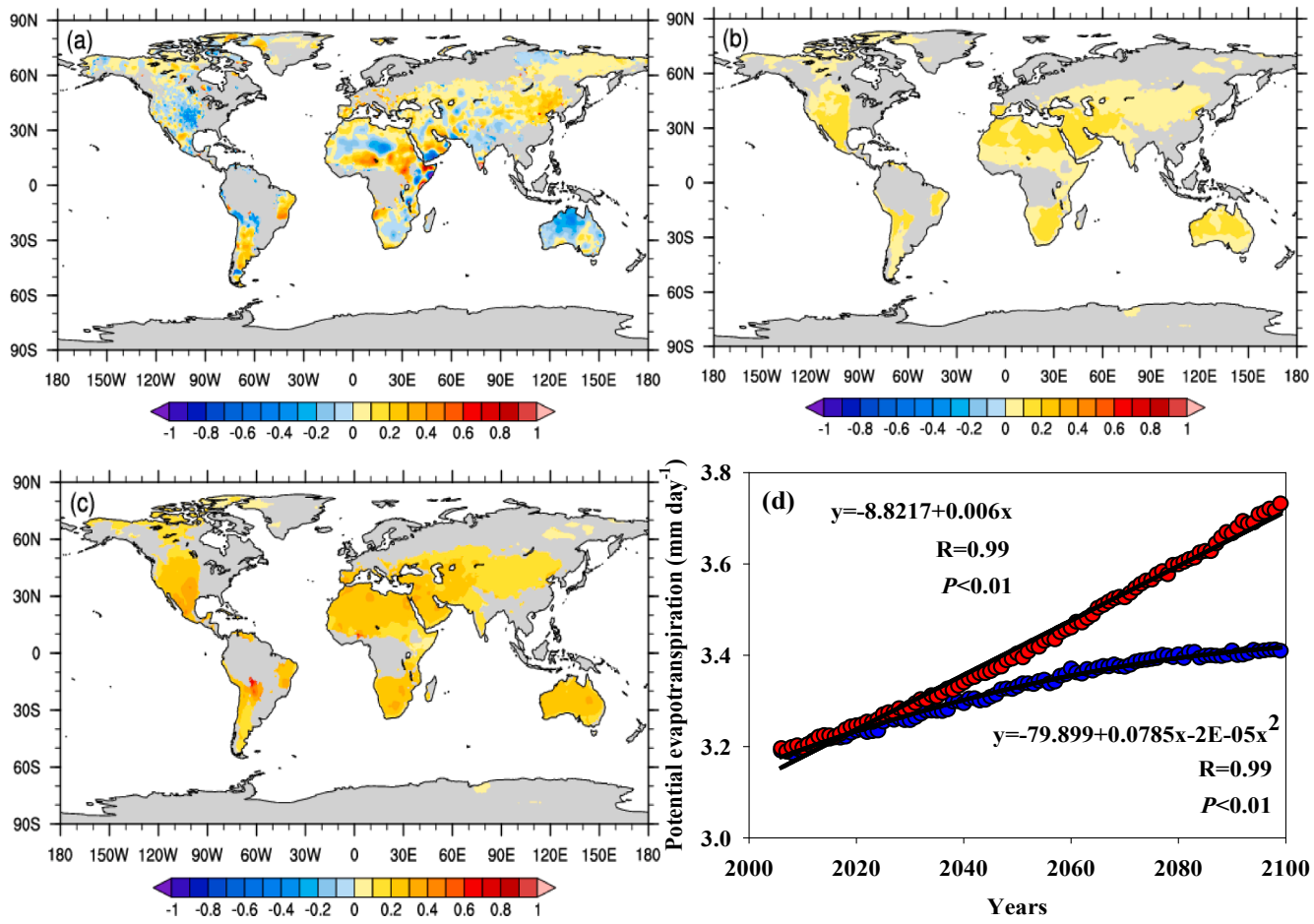

Fig. 6. Global distribution of the trend of potential evapotranspiration (mm day^{-1} 30 yr^{-1}) under the historical (a, 1948–2005), RCP4.5 (b, 2006–2099) and RCP8.5 (c, 2006–2099). Temporal variation of mean potential evapotranspiration is shown for RCP4.5 (blue) and RCP8.5 (red) in the Fig. d, respectively.

3.2. *Oxygen footprint linked to the dryland degradation*

Many studies have shown that global drylands as defined by the aridity index have degraded over the last sixty years and will continue to degrade in this century (Feng and Fu, 2013; Huang et al., 2016a, 2017b). The rising temperature and expanding drylands along with land use/cover change and other human activities may result in land desertification, which will pose a threat to global dryland ecological sustainability (Huang et al., 2017a, 2020). Because of oxygen cycle is closely related to thermal cycle, hydrological cycle, biological cycle and biogeochemical cycle (Huang et al., 2021) and plays an important indicate role in climate change and human activities, especially in fragile dryland regions (Huang et al., 2018a). Therefore, in this study, we combined the natural oxygen production and human-induced oxygen consumption to construct an oxygen footprint and make future estimates. Based on the oxygen footprint, it is important to identify these phase changes of the climate and dryland expansion for maintaining dryland ecological sustainability.

3.2.1. *Climate change phase*

Our study finds that dryland ecosystem changes with increases in O_F start with an anthropogenic 'climate change phase' characterized by AT, PRE, and PET. Under the RCP8.5 scenario, this increases in O_F is consistent with increases in AT, PRE, and PET, respectively (Figs. 4–6 and Fig. 8a-c). The O_F is associated with increase in human activities and disturbances, plays an important driver role in anthropogenic climate change. Over drylands, PRE-is highly variable and scarce (Ryan and Elsner, 2016), whereas PET, which represents the evaporative demand of the atmosphere (Huang et al., 2017a), stays relatively high due to the high AT, low soil water content or moisture condition, and abundant solar radiation over arid and arid-semiarid areas (Ji et al., 2014).

Meanwhile, previous studies also showed that the aridity has increased globally since approximately 1950 and that this drying trend may continue over the next century, owing to global warming, particularly in drylands, where enhanced warming is projected (Huang et al., 2016a; Huang et al., 2017a). These finds are consistent with that of our studies associated with O_F, the dryland ecosystems may have been altered by AT, PRE, and PET due to the drastic climate change and fragile ecosystems of drylands.

3.2.2. *Dryland expansion phase*

As O_F continues to increase, we identified a 'dryland expansion phase' characterized by changes in AI and the areal coverage of dryland (Fig. 7s and Fig. 8d). Our models project that PRE-will generally increase in dryland areas by ~2100, but PET, which plays a crucial role in the AI, is also projected to increase greatly (Fig. 5 and Fig. 6). Therefore, the large PET increase linked to rising AT (Fig. 4), and dryland expansion in the 21st century is projected (Fig. 7d).

Enhanced drought and decreased AI may aggravate the expansion of drylands by causing a greater evaporative demand and vapor pressure

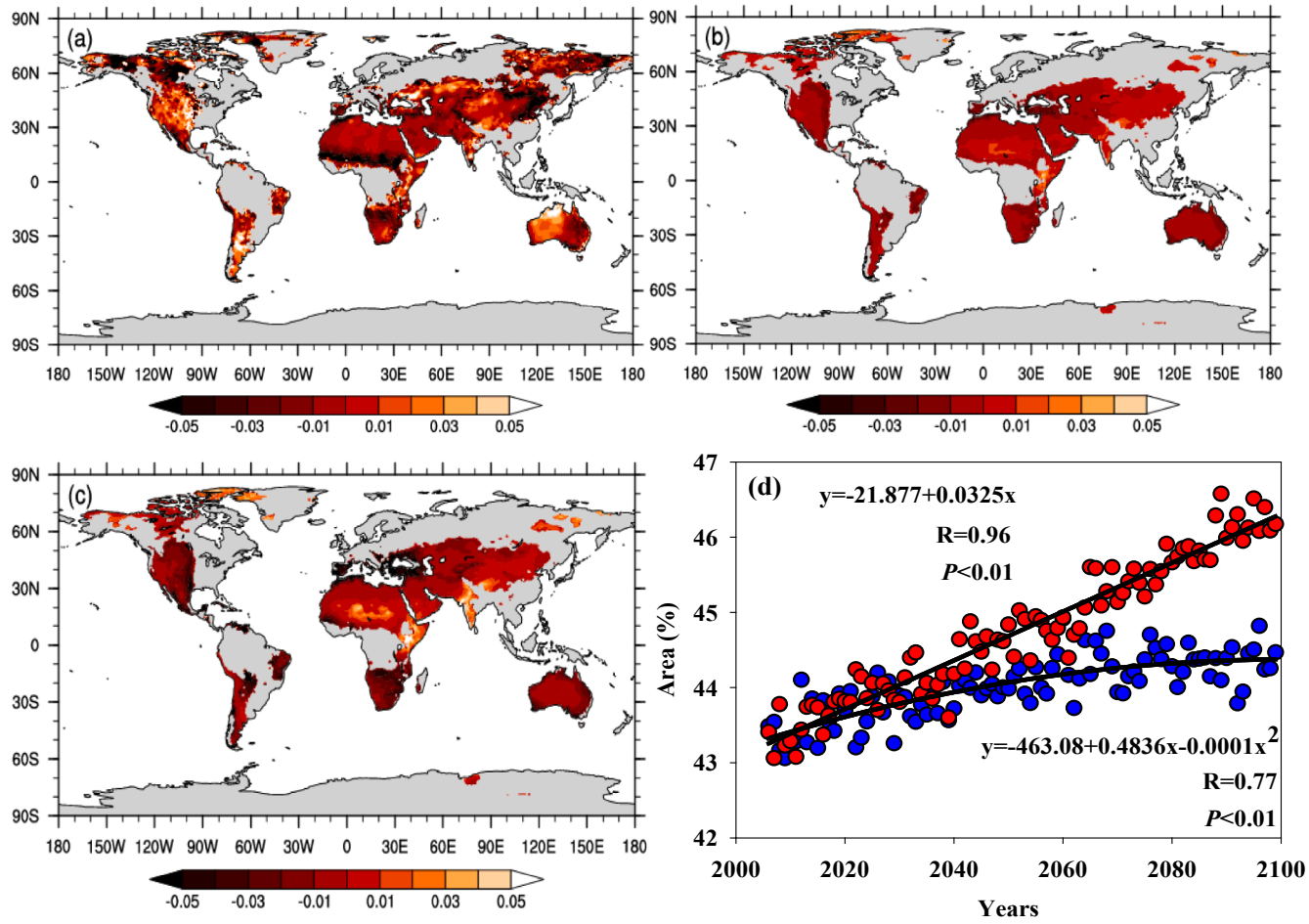

Fig. 7. Global distribution of the trend of aridity index (mm mm^{-1} 30 yr^{-1}) under the historical (a, 1948–2005), RCP4.5 (b, 2006–2099) and RCP8.5 (c, 2006–2099). Fig. d shows that temporal variation in the areal coverage of drylands (percentage of global land area) is shown for RCP4.5 (blue) and RCP8.5 (red), respectively.

deficit. Additionally, the decreased soil water content and moisture condition may lead more energy to sensible heat flux than to latent heat flux (Seneviratne et al., 2010; Sherwood and Fu, 2014), resulting in an even stronger influence on temperature extremes (Seneviratne et al., 2014; Vogel et al., 2017). Changes in AT, PRE, and PET from anthropogenic climate change are likely to affect strongly the SOC sequestration capacity in dryland areas. Thus, against the background of global-scale warming, the dryland expansion will reduce the SOC content/storage and emit CO_2 into the atmosphere (Table 1). Because of groundwater, soil moisture, and surface water deficits, dryland degradation is becoming a serious threat to terrestrial ecosystems. Thus, over drylands, O_F is important for providing useful scientific knowledge for policymakers in these areas and can serve as an indicator of anthropogenic ecosystem changes (Fig. 9).

Obviously, geoscientists can apply the oxygen footprint to investigate and reanalyze the dryland distribution, especially in dryland expansion, desertification and adaptation aspects. Because of these regions are extremely sensitive and vulnerable to climatic variability and human disturbances along with the urgent demand for regional development. Additionally, based on natural oxygen production and human-induced oxygen consumption, oxygen footprint can effectively reflect the local cool/warm conditions (Fig. 9) and therefore can act as a measure of aridity and drought changes and plays a crucial role in the evaluation and projection of global dryland ecological sustainability.

4. Conclusions

In summary, we conclude that anthropogenic ecosystem changes have significantly enhanced the oxygen footprint dynamics, affecting the land surface properties at the global scale. When production O_2 drivers are unsustainable combined with consumption O_2 drivers, this scenario will exacerbate the risk of the degradation of dryland ecosystem. Thus, we need urgent action to promote terrestrial O_2 production, including expanded the coverage of initiatives to turn marginal farmland into grassland or forest, thereby alleviating the expansion of drylands and deserts to stop dust from spreading.

In addition, improved knowledge of oxygen changes (modeling capacity and observing technology) has led to major advances in understanding global oxygen dynamics. However, we still face many challenges ahead. One key challenge is to validate model-based oxygen changes with ground observations. Currently, the lack of systematic long-term ground observation of climate and land use/cover gradients have resulted in few available ground truths to directly confirm oxygen changes detected through model products. Thus, expanding existing oxygen observational networks is a high priority.

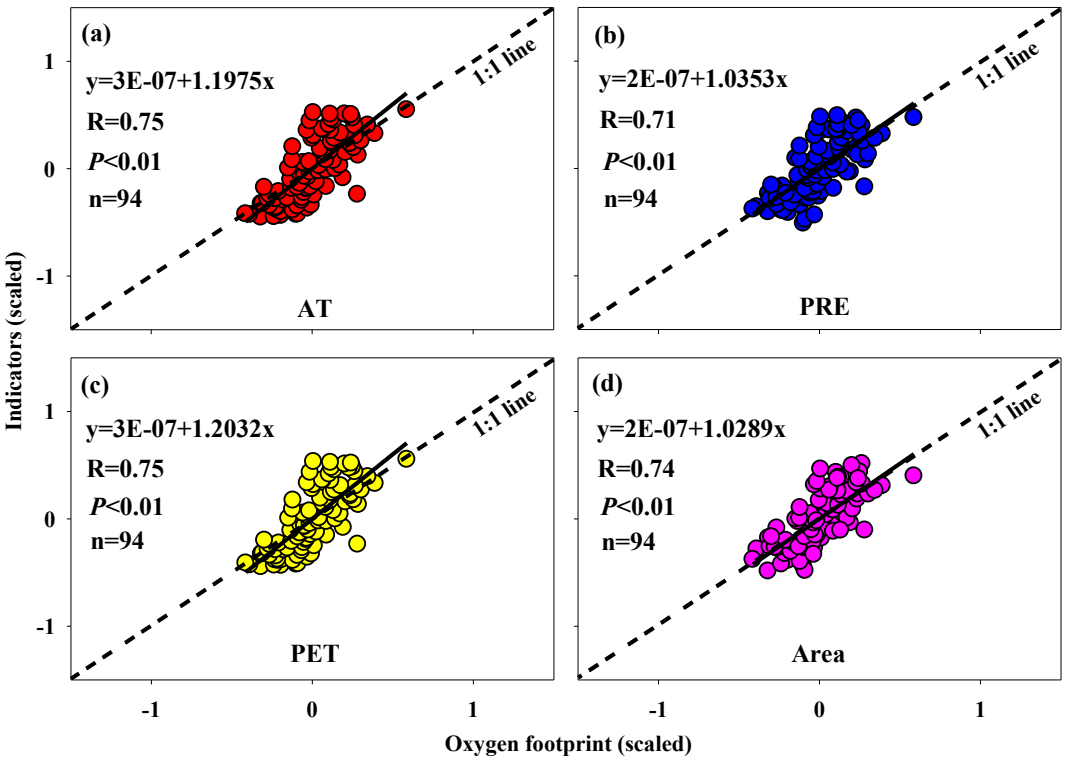

Fig. 8. The relationship between change in oxygen footprint and the indicators (a: air temperature, AT; b: precipitation, PRE; c: potential evapotranspiration, PET and d: dryland areas) under RCP8.5 scenario.

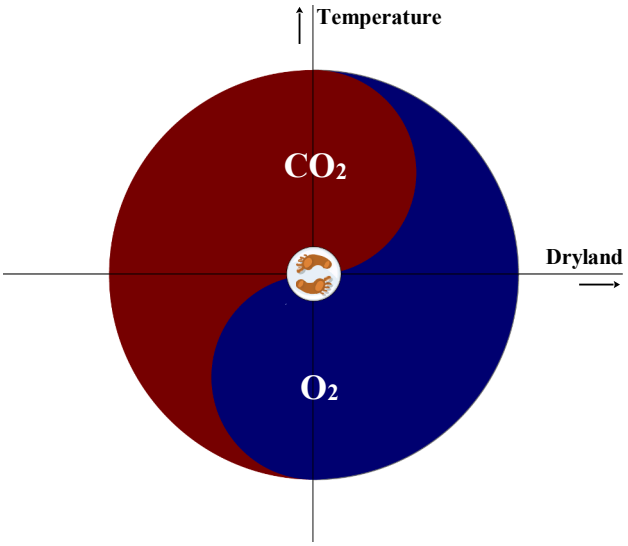

Fig. 9. The oxygen footprint based on oxygen production (O_2) and oxygen consumption (CO_2) is closely associated with dryland ecosystem degradation.

Declaration of Competing Interest

The authors declare that they have no known competing financial interests or personal relationships that could have appeared to influence the work reported in this paper.

Acknowledgment

This work was jointly supported by the National Science Foundation of China (41991231 and 41521004), the Strategic Priority Research Program of Chinese Academy of Sciences (Grant No. XDA2006010301), the China University Research Talents Recruitment Program (the '111 project', No. B13045), and Gansu Provincial Special Fund Project for Guiding Scientific and Technological Innovation and Development (2019ZX-06).We thank Y. Liu, X. Guan and Y. He for discussions and comments on the manuscript.

Data availability

The authors declare that the data supporting the results of this work are available within the paper.

References

Avila, F.B., Pitman, A.J., Donat, M.G., Alexander, L.V., Abramowitz, G., 2012. Climate model simulated changes in temperature extremes due to land cover change. J. Geophys. Res.-Atmos. 117, D04108. https://doi.org/10.1029/2011JD016382.

Barnett, J., O'Neill, S., 2010. Maladaptation. Global Environ. Change 20, 211–213. https://doi.org/10.1016/j.gloenvcha.2009.11.004.

Berdugo, M., Delgado-Baquerizo, M., Soliveres, S., Hernández-Clemente, R., Zhao, Y., Gaitán, J.J., Gross, N., Saiz, H., Maire, V., Lehman, A., Rillig, M.C., Solé, R.V., Maestre, F.T., 2020. Global ecosystem thresholds driven by aridity. Science 367, 787–790. https://doi.org/10.1126/science.aay5958.

Bond, T.C., Doherty, S.J., Fahey, D.W., Forster, P.M., Berntsen, T., DeAngelo, B.J., Flanner, M.G., Ghan, S., Karcher, B., Koch, D., Kinne, S., Kondo, Y., Quinn, P.K., Sarofim, M.C., Schultz, M.G., Schulz, M., Venkataraman, C., Zhang, H., Zhang, S., Bellouin, N., Guttikunda, S.K., Hopke, P.K., Jacobson, M.Z., Kaiser, J.W., Klimont, Z., Lohmann, U., Schwarz, J.P., Shindell, D., Storelvmo, T., Warren, S.G., Zender, C.S., 2013. Bounding the role of black carbon in the climate system: a scientific assessment. J. Geophys. Res. Atmos. 118, 5380–5552. https://doi.org/10.1002/jgrd.50171.

Brandt, M., Hiernaux, P., Rasmussen, K., Tucker, C.J., Wigneron, J.P., Diouf, A.A., Herrmann, S.M., Zhang, W.M., Kergoat, L., Mbow, C., Abel, C., Auda, Y., Fensholt, R., 2019. Changes in rainfall distribution promote woody foliage production in the Sahel. Commun. Biol. 2, 133. https://doi.org/10.1038/s42003-019-0383-9.

Cao, S.X., 2008. Why large-scale afforestation efforts in China have failed to solve the desertification problem. Environ. Sci. Technol. 42, 1826–1831. https://doi.org/10.1021/es0870597.

Chen, C., Park, T., Wang, X., Piao, S., Xu, B., Chaturvedi, R.K., Fuchs, R., Brovkin, V., Ciais, P., Fensholt, R., TØmmervik, H., Bala, G., Zhu, Z., Nemani, R.R., Myneni, R.B.,

2019. China and India lead in greening of the world through land-use management. Nature Sustainability 2, 122-129. https://doi.org/10.1038/s41893-019-0220-7.
Chen, M.Y., Xie, P.P., Janowiak, J.E., Arkin, P.A., 2002. Global land precipitation: a 50-yr monthly analysis based on gauge observation. J. Hydrometeorol. 3, 249–266. https://doi.org/10.1175/1525-7541(2002)003<0249:GLPAYM>2.0.CO;2.
Cheng, J.H., Chu, P.F., Chen, D.M., Bai, Y.F., 2016. Functional correlations between specific leaf area and specific root length along a regional environmental gradient in Inner Mongolia grasslands. Funct. Ecol. 30, 985–997. https://doi.org/10.1111/1365-2435.12569.
Crutzen, P.J., 2002. Geology of mankind. Nature 415, 23. https://doi.org/10.1038/415023a.
Dardel, C., Kergoat, L., Hiernaux, P., Mougin, E., Grippa, M., Tucker, C.J., 2014. Re-greening Sahel: 30 years of remote sensing data and field observations (Mali, Niger). Remote Sens. Environ. 140, 350–364. https://doi.org/10.1016/j.rse.2013.09.011.
Fan, Y., Dool, H.V.D.A., 2008. A global monthly land surface air temperature analysis for 1948-present. J. Geophys. Res. 113, D01103. https://doi.org/10.1029/2007JD008470.
Farquhar, G.D., Sharkey, T.D., 1982. Stomatal conductance and photosynthesis. Annu. Rev. Plant Physiol. 33, 317–345. https://doi.org/10.1146/annurev. pp.33.060182.001533.
Feng, S., Fu, Q., 2013. Expansion of global drylands under a warming climate. Atmos. Chem. Phys. 13, 10081–10094. https://doi.org/10.5194/acp-13-10081-2013.
Fensholt, R., Langanke, T., Rasmussen, K., Reenberg, A., Prince, S.D., Tucker, C., Scholes, R.J., Le, Q.B., Bondeau, A., Eastman, R., Epstein, H., Gaughan, A.E., Hellden, U., Mbow, C., Olsson, L., Paruelo, J., Schweitzer, C., Seaquist, J., Wessels, K., 2012. Greenness in semi-arid areas across the globe 1981–2007-An Earth Observing Satellite based analysis of trends and drivers. Remote Sens. Environ. 121, 144–158. https://doi.org/10.1016/j.rse.2012.01.017.
Fu, Q., Feng, S., 2014. Responses of terrestrial aridity to global warming. J. Geophys. Res.: Atmos. 119, 7863–7875. https://doi.org/10.1002/2014JD021608.
Gray, S.B., Dermody, O., Klein, S.P., Locke, A.M., McGrath, J.M., Paul, R.E., Rosenthal, D. M., Ruiz-Vera, U.M., Siebers, M.H., Strellner, R., Ainsworth, E.A., Bernacchi, C.J., Long, S.P., Ort, D.R., Leakey, A.D.B., 2016. Intensifying drought eliminates the expected benefits of elevated carbon dioxide for soybean. Nat. Plants 2, 16132. https://doi.org/10.1038/NPLANTS.2016.132.
Guan, X., Ma, J., Huang, J., Huang, R., Zhang, L., Ma, Z., 2019. Impact of oceans on climate change in drylands. Sci. China-Earth Sci. 62, 891–908. https://doi.org/10.1007/s11430-018-9317-8.
Herrmann, S.M., Anyamba, A., Tucker, C.J., 2005. Recent trends in vegetation dynamics in the African Sahel and their relationship to climate. Global Environ. Change 15, 394–404. https://doi.org/10.1016/j.gloenvcha.2005.08.004.
Huang, J., Yu, H., Guan, X., Wang, G., Guo, R., 2016a. Accelerated dryland degradation under climate change. Nat. Clim. Change 6, 166–172. https://doi.org/10.1038/nclimate2837.
Huang, J., Ji, M., Xie, Y., Wang, S., He, Y., Ran, J., 2016b. Global semi-arid climate change over last 60 years. Clim. Dyn. 46, 1131–1150. https://doi.org/10.1007/s00382-015-2636-8.
Huang, J., Li, Y., Fu, C., Chen, F., Fu, Q., Dai, A., Shinoda, M., Ma, Z., Guo, W., Li, Z., Zhang, L., Liu, Y., Yu, H., He, Y., Xie, Y., Guan, X., Ji, M., Lin, L., Wang, S., Yan, H., Wang, G., 2017a. Dryland climate change: recent progress and challenges. Rev. Geophys. 55, 587–854. https://doi.org/10.1002/2016RG000550.
Huang, J., Yu, H., Dai, A., Wei, Y., Kang, L., 2017b. Drylands face potential threat under 2 ℃ global warming target. Nat. Clim. Change 7, 417–422. https://doi.org/10.1038/NCLIMATE3275.
Huang, J., Huang, J., Liu, X., Li, C., Ding, L., Yu, H., 2018a. The global oxygen budget and its future projection. Sci. Bull. 63, 1180–1186. https://doi.org/10.1016/j.scib.2018.07.023.
Huang, K., Xia, J., Wang, Y., Ahlström, A., Chen, J., Cook, R.B., Cui, E., Fang, Y., Fisher, J.B., Huntzinger, Deborah Nicole, Li, Z., Michalak, A.M., Qiao, Y., Schaefer, K., Schwalm, C., Wang, J., Wei, Y., Xu, X., Yan, L., Bian, C., Luo, Y., 2018b. Enhanced peak growth of global vegetation and its key mechanisms. Nat. Ecol. Evolut. 2, 1897–1905. https://doi.org/10.1038/s41559-018-0714-0.
Huang, J., Yu, H., Han, D., Zhang, G., Wei, Y., Huang, J., An, L., Liu, X., Ren, Y., 2020. Declines in global ecological security under climate change. Ecol. Ind. 117, 106651. https://doi.org/10.1016/j.ecolind.2020.106651.
Huang, J., Liu, X., He, Y., Shen, S., Hou, Z., Li, S., Li, C., Yao, L., Huang, J., 2021. The oxygen cycle and a habitable Earth. Sci. China Earth Sci. 64, 511–528. https://doi.org/10.1007/s11430-020-9747-1.
Hulme, M., 1996. Recent climatic change in the world's drylands. Geophys. Res. Lett. 23, 61–64. https://doi.org/10.1029/95GL03586.
Jansson, J.K., Homfmockel, K.S., 2020. Soil microbiomes and climate change. Nat. Rev. Microbiol. 18, 35–46. https://doi.org/10.1038/s41579-019-0265-7.
Ji, F., Wu, Z.H., Huang, J.P., Chassignet, E.P., 2014. Evolution of land surface air temperature trend. Nat. Clim. Change 4, 462–466. https://doi.org/10.1038/nclimate2223.
Junkermann, W., Hacker, J., Lyons, T., Nair, U., 2009. Land use change suppresses precipitation. Atmos. Chem. Phys. 9, 6531–6539. https://doi.org/10.5194/acp-9-6531-2009.
Keeling, R.F., 1988. Measuring correlations between atmospheric oxygen and carbon dioxide mole fractions: a preliminary study in urban air. J. Atmos. Chem. 7, 153–176. https://doi.org/10.1007/BF00048044.
Keenan, T.F., Hollinger, D.Y., Bohrer, G., Dragoni, D., Munger, J.W., Schmid, H.P., Richardson, A.D., 2013. Increase in forest water-use efficiency as atmospheric carbon dioxide concentrations rise. Nature 499, 324–327. https://doi.org/10.1038/nature12291.
Lehmann, J., Kleber, M., 2015. The contentious nature of soil organic matter. Nature 528, 60–68. https://doi.org/10.1038/nature16069.
Li, C., Zhao, T., Ying, K., 2015. Effects of anthropogenic aerosols on temperature changes in China during the twentieth century based on CMIP5 models. Theor. Appl. Climatol. 125, 529–540. https://doi.org/10.1007/s00704-015-1527-6.
Lin, L., Gettelman, A., Fu, Q., Xu, Y., 2018. Simulated differences in 21st century aridity due to different scenarios of greenhouse gases and aerosols. Clim. Change 146, 407–422. https://doi.org/10.1007/s10584-016-1615-3.
Liu, X.Y., Huang, J.P., Huang, J.P., Li, C.Y., Ding, L., Meng, W.J., 2020. Estimation of gridded atmospheric oxygen consumption from 1975 to 2018. J. Meteorolog. Res. 34, 1–13. https://doi.org/10.1007/s13351-020-9133-7.
Mackey, B., Prentice, I.C., Steffen, W., House, J.I., Lindenmayer, D., Keith, H., Berry, S., 2013. Untangling the confusion around land carbon science and climate change mitigation policy. Nat. Clim. Change 3, 552–557. https://doi.org/10.1038/nclimate1804.
Marvel, K., Cook, B.I., Bonfils, C.J.W., Durack, P.J., Smerdon, J.E., Williams, A.P., 2019. Twentieth- century hydroclimate changes consistent with human influence. Nature 569, 59–65. https://doi.org/10.1038/s41586-019-1149-8.
Oke, T.R., 1987. Boundary layer climates. New York: Methuen. https://doi.org/10.2307/214824.
Piao, S., Wang, X., Park, T., Chen, C., Lian, X., He, Y., Bjerke, J. W., Chen, A., Ciais, P., TØmmervik, H., Nemani, R.R., Myneni, R.B., 2020. Characteristics, drivers and feedbacks of global greening. Nature Rev. Earth Environ. 1, 14-27. https://doi.org/10.1038/s43017-019-0001-x.
Piao, S.L., Yin, G.D., Tan, J.G., Cheng, L., Huang, M.T., Li, Y., Liu, R.G., Mao, J.F., Myneni, R.B., Peng, S.S., Poulter, B., Shi, X.Y., Xiao, Z.Q., Zeng, N., Zeng, Z.Z., Wang, Y.P., 2015. Detection and attribution of vegetation greening trend in China over the last 30 years. Global Change Biology 21, 1601-1609. https://doi.org/doi:10.1111/gcb.12795.
Poulsen, C.J., Tabor, C., White, J.D., 2015. Long-term climate forcing by atmospheric oxygen concentrations. Science 348, 1238-1241. https://doi.org/10.1126/science.1260670.
Reich, P.B., Hobbie, S.E., 2013. Decade-long soil nitrogen constraint on the CO_2 fertilization of plant biomass. Nat. Clim. Change 3, 278–282. https://doi.org/10.1038/NCLIMATE1694.
Reich, P.B., Hobbie, S.E., Lee, T.D., 2014. Plant growth enhancement by elevated CO_2 eliminated by joint water and nitrogen limitation. Nat. Geosci. 7, 920–924. https://doi.org/10.1038/NGEO2284.
Reynolds, J.F., Stafford Smith, D.M., Lambin, E.F., Turner, B.L., Mortimore, M., Batterbury, S.P.J., Downing, T.E., Dowlatabadi, H., Fernandez, R.J., Herrick, J.E., Huber-Sannwald, E., Jiang, H., Leemans, R., Lynam, T., Maestre, F.T., Ayarza, M., Walker, B., 2007. Global desertification: Building a science for dryland development. Science 316, 847–851. https://doi.org/10.1126/science.1131634.
Ryan, C., Elsner, P., 2016. The potential for sand dams to increase the adaptive capacity of East African drylands to climate change. Reg. Environ. Change 16, 2087–2096. https://doi.org/10.1007/s10113-016-0938-y.
Seneviratne, S.I., Corti, T., Davin, E.L., Hirschi, M., Jaeger, E.B., Lehner, I., Orlowsky, B., Teuling, A.J., 2010. Investigating soil moisture-climate interactions in a changing climate: a review. Earth Sci. Rev. 99, 125–161. https://doi.org/10.1016/j.earscirev.2010.02.004.
Seneviratne, S.I., Donat, M.G., Mueller, B., Alexander, L.V., 2014. No pause in the increase of hot temperature extremes. Nat. Clim. Change 4, 161–163. https://doi.org/10.1038/nclimate2145.
Sherwood, S., Fu, Q., 2014. A drier future? Science 343, 737–739. https://doi.org/10.1126/science.1247620.
Steinbach, J., Gerbig, C., Rödenbeck, C., Karstens, U., Minejima, C., Mukai, H., 2011. The CO_2 release and oxygen uptake from fossil fuel emission estimate (COFFEE) dataset: effects from varying oxidative ratios. Atmos. Chem. Phys. 11, 6855–6870. https://doi.org/10.5194/acp-11-6855-2011.
Taylor, C.M., Lambin, E.F., Stephenne, N., Harding, R.J., Essery, R.L.H., 2002. The influence of land use change on climate in the Sahel. J. Clim. 15, 3615–3629. https://doi.org/10.1175/1520-0442(2002)015<3615:TIOLUC>2.0.CO;2.
Taylor, K.E., Stouffer, R.J., Meehl, G.A., 2012. An overview of CMIP5 and the experiment design. Bull. Am. Meteorol. Soc. 4, 485–498. https://doi.org/10.1175/BAMS-D-11-00094.1.
van der Werf, G.R., Randerson, J.T., Giglio, L., van Leeuwen, T.T., Chen, Y., Rogers, B.M., Mu, M.Q., van Marle, M.J.E., Morton, D.C., Collatz, G.J., Yokelson, R.J., Kasibhatla, P.S., 2017. Global fire emissions estimates during 1997–2016. Earth Syst. Sci. Data 9, 697–720. https://doi.org/10.5194/essd-9-697-2017.
Vogel, M.M., Orth, R., Cheruy, F., Hagemann, S., Lorenz, R., van den Hurk, B.J.J.M., Seneviratne, S.I., 2017. Regional amplification of projected changes in extreme temperatures strongly controlled by soil moisture-temperature feedbacks. Geophys. Res. Lett. 44, 1511–1519. https://doi.org/10.1002/2016GL071235.
Wang, J., Song, C., Reager, J.T., Yao, F., Famiglietti, J.S., Sheng, Y., MacDonald, G.M., Brun, F., Schmied, Hannes Müller, Marston, R.A., Wada, Y., 2018. Recent global decline in endorheic basin water storages. Nat. Geosci. 11, 926–932. https://doi.org/10.1038/s41561-018-0265-7.
Xia, J., Wan, S.Q., 2008. Global response patterns of terrestrial plant species to nitrogen addition. New Phytol. 179, 428–439. https://doi.org/10.1111/j.1469-8137.2008.02488.x.
Yan, Z.F., Bond-Lamberty, B., Todd-Brown, K.E., Bailey, V.L., Li, S., Liu, C.Q., Liu, C., 2018. A moisture function of soil heterotrophic respiration that incorporates microscale processes. Nat. Commun. 9, 2562. https://doi.org/10.1038/s41467-018-04971-6.

Yao, J., Liu, H., Huang, J., Gao, Z., Wang, G., Li, D., Yu, H., Chen, X., 2020. Accelerated dryland expansion regulates future variability in dryland gross primary production. Nat. Commun. 11, 1665. https://doi.org/10.1038/s41467-020-15515-2.

Yu, P.J., Han, K.X., Li, Q., Zhou, D.W., 2017. Soil organic carbon fractions are affected by different land uses in an agro-pastoral transitional zone in Northeastern China. Ecol. Ind. 73, 331–337. https://doi.org/10.1016/j.ecolind.2016.10.002.

Zaehle, S., Medlyn, B.E., De Kauwe, M.G., Walker, A.P., Dietze, M.C., Hickler, T., Luo, Y. Q., Wang, Y.P., El-Masri, B., Thornton, P., Jain, A., Wang, S.S., Warlind, D., Weng, E. S., Parton, W., Iversen, C.M., Gallet-Budynek, A., McCarthy, H., Finzi, A.C., Hanson, P.J., Prentice, I.C., Oren, R., Norby, R.J., 2014. Evaluation of 11 terrestrial carbon-nitrogen cycle models against observations from two temperature Free-Air CO_2 Enrichment studies. New Phytol. 202, 803–822. https://doi.org/10.1111/nph.12697.

Zhang, K., Zheng, H., Chen, F.L., Ouyang, Z.Y., Wang, Y., Wu, Y.F., Lan, J., Fu, M., Xiang, X.W., 2015. Changes in soil quality after converting Pinus to Eucalyptus plantations in southern China. Soil Earth 6, 115–123. https://doi.org/10.5194/se-6-115-2015.

Zhu, Z., Piao, S., Myneni, R.B., Huang, M., Zeng, Z., Canadell, J.G., Ciais, P., Sitch, S., Friedlingstein., P., Arneth, A., Cao, C., Cheng, L., Kato, E., Koven, C., Li, Y., Lian, X., Liu, Y., Liu, R., Mao, J., Pan, Y., Peng, S., Peñuelas, J., Poulter, B., Pugh, T.A.M., Stocker, B.D., Viovy, N., Wang, X., Wang, Y., Xiao, Z., Yang, H., Zaehle, S., Zeng, N., 2016. Greening of the Earth and its drivers. Nat. Clim. Change 6, 791-795. https://doi.org/10.1038/ nclimate3004.